Concurrent atomization and phase change in a multicomponent liquid: Modeling and analysis

Josette Bellan
Jet Propulsion Laboratory, California Institute of Technology

Abstract

A model has been developed to account for the occurrence of concurrent atomization of a fully multi-species liquid and phase change from liquid to vapor. The model is based on the concepts of Continuous Thermodynamics in which the composition is treated statistically through a probability distribution function. The liquid and the gas phase have compositions which evolve spatially and temporally. The surface between liquid and gas is tracked using the level-set method. An analysis of the conservation equations is here performed that allows the definition of novel effective non-dimensional numbers to assess the scales at which composition changes compared to viscous effects which dominate atomization through the surface tension. An effective Prandtl number is also derived to assess heating effects leading to phase change compared to viscous effects. These non-dimensional numbers should be computed in the future, once simulations of these flows are available. Their values will be of engineering interest to determine the ratio of characteristic times for compositional and viscosity-induced changes, and for heat transfer in a complex mixture compared to viscosity-induced changes.

1 Introduction

Liquid fuel atomization models and simulations all assume that the resulting drops have the same composition as the injected fuel. This is certainly correct for single-species fuels. However, when a fuel which is a complex mixture of chemical species is injected into a hot combustion chamber, it is subjected to two competing phenomena: (1) evaporation of chemical species from the liquid-jet surface, and (2) rupture of the liquid-jet surface into filaments and drops – atomization. If evaporation is faster than atomization, the compositions of these drops will differ significantly from that of the injected fuel. This difference will impact calculations of ignition, flame stability and pollutant formation. Given the fact that current fuels such as kerosenes, diesel, RP-1, JP7 are complex mixtures of many species and that the same holds for biofuels which are becoming increasingly of aeronautics interest, it is imperative to investigate

the result of concurrent evaporation and atomization of multicomponent fuels. We note that whereas there is testing experience of many years with kerosenes and their behavior is well known [5], there is practically no such experience with biofuels which are increasingly being used. Applying the present model to kerosenes would validate the model's physical realism and permit expressing confidence that it has the potential to portray the unknown behavior of biofuels. Developing models and computational methods to address complex compositions is essential since experimental methods are currently in infancy compared to engineering needs (e.g. [18]).

This study is devoted to developing such a model and then analyzing the model equations to gain further insight into the governing phenomena according to the fuel composition. Figure 1 illustrates the contrast between the commonly used representation of the composition based upon individual species (figure 1a) and the present continuous composition representation (figure 1b) which is the cornerstone of the present model. Clearly, as the number of species increases, it is computationally impractical to consider the composition based upon individual species since the model becomes increasingly computationally intensive. In contrast, considering the composition statistically greatly reduces the computational burden while maintaining accuracy [9]. The model for the governing equations are described in §2 and their analysis in §3. A summary and conclusions are offered in §4.

2 Governing Equations

The model is built in the framework of Continuous Thermodynamics (CT) [4, 6]. In CT, the chemical potential for a mixture containing numerous components is appropriately represented, and the Gibbs function is derived through molecular thermodynamic methods in terms of the probability distribution function (PDF) describing the mixture composition. The concepts are fundamental and independent of the physicochemical model chosen for the chemical potential. From a specified initial PDF, the evolution of the mixture is determined by the physics of the situation encapsulated into thermodynamic relationships and/or conservation equations. Albeit the composition PDF generally depends on many variables, it can be appropriately chosen to depend on one or a restricted number of variables that govern the phenomena under consideration. For example, it has been shown, with validation, that the single-Gamma PDF (SGPDF) depending on the molar weight, m, can represent an entire homologous species class of hydrocarbons [3, 4, 15, 17].

In CT form, the mole fraction of a discrete species k is defined by the value of a continuous distribution function, P, in the vicinity of the molar mass coordinate corresponding to that species

$$X_{kl} = P_l(m_k)\Delta m_k \tag{1}$$

$$X_{kv} = X_v P_v(m_k)\Delta m_k. \tag{2}$$

The multicomponent (MC) drop model of [9] is adopted wherein the MC liquid composition and gas composition in the vicinity of the drop surface are described by

$$P(m;\alpha_1,\beta_1,\alpha_2,\beta_2,\varepsilon) = (1-\varepsilon)f_\Gamma^{(1)} + \varepsilon f_\Gamma^{(2)}, \tag{3}$$

where $f_\Gamma^{(k)} = f_\Gamma(m;\alpha_k,\beta_k)$ with integer $k = 1, 2$, ε is a weighting parameter ($0 \leqslant \varepsilon \leqslant 1$), $\int_\gamma^\infty P(m)dm = 1$ and

$$f_\Gamma(m) = \frac{(m-\gamma)^{\alpha-1}}{\beta^\alpha \Gamma(\alpha)} \exp\left[-\left(\frac{m-\gamma}{\beta}\right)\right] \tag{4}$$

where $\Gamma(\alpha)$ is the Gamma function and $f_\Gamma(m)$ is a SGPDF. The origin of f is specified by γ which is the molar mass of the smallest molar-mass species in the mixture ($P(m;\alpha_1,\beta_1,\alpha_2,\beta_2,\varepsilon)$ was developed in [9] with $\gamma_1 = \gamma_2 = \gamma$), and its shape is determined by α and β. At each time t, $P(m;\alpha_1,\beta_1,\alpha_2,\beta_2,\varepsilon)$, which is called a Double Gamma PDF (DGPDF), is determined by the vector $\boldsymbol{\eta} \equiv (\alpha_1,\beta_1,\alpha_2,\beta_2,\varepsilon)$. According to [9], P can be determined by an inverse mapping from its first four moments, ξ_n where integer $n \in [1, 4]$, with a fifth parameter empirically calculated. These moments are defined as

$$\xi_{nl} \equiv \int_\gamma^\infty m^n P_l(m)dm,\ \xi_{nv} \equiv \int_\gamma^\infty m^n P_v(m)dm, \tag{5}$$

for integer $n \geqslant 1$, where subscripts l and v denote the liquid and vapor, respectively. Although in the vicinity of each drop surface the vapor composition is represented by P_v according to equation (3), away from the drops the mathematical form of P_v is determined by the vapor released from the drops and by gaseous mixing. At each t, P_l describes the liquid-fuel composition, which is specific to each drop, and P_v describes the vapor composition, which varies with spatial location. Throughout this paper we adopt the notation $\theta \equiv \xi_1$ and $\psi \equiv \xi_2$, and the standard deviation of P is calculated as $\sigma = \sqrt{(\psi - \theta^2)}$. Also following [9], one can define ξ_n^{SGPDF} as being the moments of a SGPDF that would have the same ξ_1 and ξ_2 values as a specified P. Thus, 'excess moments' of any PDF P with respect to the SGPDF that has the same θ and ψ as P are defined by

$$\xi_n' \equiv \xi_n - \xi_n^{SGPDF}. \tag{6}$$

By definition $\xi_1' = \xi_2' = 0$ and a DGPDF then corresponds to $\xi_n' \neq 0$ for $n \geqslant 3$. Deviation of any PDF from the equivalent SGPDF decreases with decreasing (ξ_n'/ξ_n^{SGPDF}).

The difference between the models of [9, 11] and the present model is that in those studies *it had already been assumed that drops were formed,* and thus there was no model of liquid atomization. Basically, assuming that drops exist entirely eliminates considerations of surface tension because its role is solely to determine the curvature of the liquid surface. In contrast, when inquiring about atomization, the surface tension and the force it generates are prominent quantities determining the

fate of the liquid. This difference between the current and previous work should not be trivialized because it is pivotal to the present model of concurrent atomization and phase change.

2.1 Liquid-phase equations

We assume that there are negligible solubility effects of gas into the liquid, an assumption justified at the atmospheric pressure under consideration. The liquid is followed in an Eulerian frame and the generic conservation equations for continuity, momentum, energy, species and PDF first four moments (θ_l, ψ_l, ξ_{3l}, ξ_{4l}) representing the composition are:

$$\frac{\partial \Phi_l}{\partial t} + \frac{\partial \left[\Phi_l u_{lj}\right]}{\partial x_j} = \frac{\partial \left[\Psi_l(\Phi_l)\right]}{\partial x_j}, \tag{7}$$

where

$$\Phi_l = \{c_l,\ c_l m_l u_{li},\ c_l m_l e_{lt},\ c_l \theta_l,\ c_l \psi_l,\ c_l \xi_{3l},\ c_l \xi_{4l}\} \tag{8}$$

is the vector of the conservative variables,

$$\begin{aligned}\Psi_l(\Phi_l) = \{&c_l m_l \mathcal{D}_l \frac{\partial}{\partial x_j}\left(\frac{1}{m_l}\right),\ \ -p_l\delta_{ij} + \sigma_{lij},\\ &-p_l u_{lj} + u_{li}\sigma_{lij} + \lambda_l \frac{\partial T_l}{\partial x_j} + \alpha_1(T_l)\frac{\partial}{\partial x_j}\left(\frac{1}{m_l}\right) + \alpha_2(T_l)\frac{\partial}{\partial x_j}\left(\frac{\theta_l}{m_l}\right) + \alpha_3 \frac{\partial}{\partial x_j}\left(\frac{\psi_l}{m_l}\right),\\ &c_l m_l \mathcal{D}_{l,\xi 1}\frac{\partial}{\partial x_j}\left(\frac{\theta_l}{m_l}\right), c_l m_l \mathcal{D}_{l,\xi 2}\frac{\partial}{\partial x_j}\left(\frac{\psi_l}{m_l}\right), c_l m_l \mathcal{D}_{l,\xi 3}\frac{\partial}{\partial x_j}\left(\frac{\xi_{3l}}{m_l}\right),\\ &c_l m_l \mathcal{D}_{l,\xi 4}\frac{\partial}{\partial x_j}\left(\frac{\xi_{4l}}{m_l}\right)\}\end{aligned} \tag{9}$$

is the diffusional flux vector corresponding to Φ_l. Because the liquid is entirely composed of fuel (we do not consider solubility effects, as this study is performed under the condition of atmospheric pressure), the liquid mass density $\rho_l = c_l m_l$ and $m_l = \theta_l$. In equations (7)-(9) c_l is the liquid molar density, x_i is the i^{th} spatial coordinate, $\mathbf{u}_l$ is the liquid mass-averaged velocity, $\mathcal{D}_l$ is an effective diffusion coefficient defined as the proportionality coefficient between the liquid mass flux and $c_l m_l \nabla(1/m_l)$ (that is, the liquid mass may change as a consequence of the changing composition) which turns out to be

$$\mathcal{D}_l = \int_{\gamma_v}^{\infty} D(m,T) P_l(m) dm, \tag{10}$$

by definition

$$\mathcal{D}_{l,\xi n}\xi_{nl} = \int_{\gamma_v}^{\infty} D(m,T) P_l(m) m^n dm \tag{11}$$

where

$$D(m,T) = (A_D + B_D m) T^{5/2}/(B_\Phi + T) \tag{12}$$

which can approximate the diffusional behavior of the α-species in the mixture; constants A_D, B_D and B_Φ are listed in [16], p_l is the pressure inside the liquid, σ_{lij} is the viscous stress tensor, δ_{ij} is the Kronecker symbol, $e_{lt} = e_{lk} + e_{lint} = u_{li}u_{li}/2 + h_l - p_l/\rho_l$ is the total energy of the liquid, h is the enthalpy, λ_l is the liquid thermal conductivity and T_l is the liquid temperature. For simplicity, ρ_l is assumed constant (effectively $\rho_l = \rho_{l,0}$ is the liquid-phase equation of state where the subscript 0 denotes the initial condition), an assumption which is most likely very good as a first approximation, particularly since we do not consider solubility effects.

2.2 Gas-phase equations

The gas is followed in an Eulerian frame and the generic conservation equations for continuity, momentum, energy, species and PDF first four moments $(\theta_v, \psi_v, \xi_{3v}, \xi_{4v})$ representing the vapor composition are

$$\frac{\partial \Phi_g}{\partial t} + \frac{\partial \left[\Phi_g u_{gj}\right]}{\partial x_j} = \frac{\partial \left[\Psi_g(\Phi_g)\right]}{\partial x_j}, \tag{13}$$

where

$$\Phi_g = \{c_g,\ c_g m_g u_{gi},\ c_g m_g e_{gt},\ c_g X_v,\ c_g X_v \theta_v,\ c_g X_v \psi_v,\ c_g X_v \xi_{3v},\ c_g X_v \xi_{4v}\} \tag{14}$$

is the vector of the conservative variables,

$$\begin{aligned}\Psi_g(\Phi_g) = \{&c_g m_g \mathcal{D}_g \frac{\partial}{\partial x_j}\left[\frac{X_v}{m_g}\left(1 - \frac{\theta_v}{m_a}\right)\right],\ -p_g\delta_{ij} + \sigma_{gij},\\ &-p_g u_j + u_{gi}\sigma_{ij} + \lambda_g \frac{\partial T_g}{\partial x_j} + \alpha_1(T_g)\frac{\partial}{\partial x_j}\left(\frac{X_v}{m_g}\right) + \alpha_2(T_g)\frac{\partial}{\partial x_j}\left(\frac{X_v\theta_v}{m_g}\right)\\ &+ \alpha_3 \frac{\partial}{\partial x_j}\left(\frac{X_v\psi_v}{m_g}\right), c_g m_g \mathcal{D}_g \frac{\partial}{\partial x_j}\left(\frac{X_v}{m_g}\right), c_g m_g \mathcal{D}_{g,\xi 1}\frac{\partial}{\partial x_j}\left(\frac{X_v\theta_v}{m_g}\right),\\ &c_g m_g \mathcal{D}_{g,\xi 2}\frac{\partial}{\partial x_j}\left(\frac{X_v\psi_v}{m_g}\right), c_g m_g \mathcal{D}_{g,\xi 3}\frac{\partial}{\partial x_j}\left(\frac{X_v\xi_{3v}}{m_g}\right), c_g m_g \mathcal{D}_{g,\xi 4}\frac{\partial}{\partial x_j}\left(\frac{X_v\xi_{4v}}{m_g}\right)\}\end{aligned} \tag{15}$$

is the diffusional flux vector corresponding to Φ_g. In equations (13)-(15) c_v is the molar density, x_i is the i^{th} spatial coordinate, $\mathbf{u}_v$ is the mass-averaged velocity,

$$m_g = \theta_v X_v + m_a(1 - X_v) \tag{16}$$

is the molar mass where m_a is the carrier gas molar mass (subscript a denotes the carrier gas) and $\theta_v X_v = m_v$, $\mathcal{D}_g$ is an effective diffusion coefficient defined by [8] as the proportionality coefficient between the vapor mass flux and $c_g m_g \nabla(X_v/m_g)$, p_g is the pressure, σ_{gij} is the viscous stress tensor, δ_{ij} is the Kronecker symbol, $e_{gt} = e_{gk} + e_{gint} = u_{gi}u_{gi}/2 + h_g - p_g/\rho_g$ is the total energy of the gas, $\rho_g = m_g c_g$

is the mass density, h_g is the enthalpy, λ_g is the thermal conductivity and T_g is the gas temperature. The last three terms of the heat flux in the energy equation are the portion due to transport of species by the molar fluxes; the detailed expressions for $\alpha_1(T), \alpha_2(T)$ and α_3 are presented in Appendix 1. Similar to definitions for the liquid,

$$\mathcal{D}_g = \int_{\gamma_v}^{\infty} D(m,T) P_g(m) dm, \tag{17}$$

by definition

$$\mathcal{D}_{g,\xi^n} \xi_{ng} = \int_{\gamma_v}^{\infty} D(m,T) P_g(m) m^n dm \tag{18}$$

with $D(m,T)$ defined by equation (12).

The perfect gas equation of state (EOS)

$$p = (\rho R_u T)/m = c R_u T \tag{19}$$

where R_u is the universal gas constant, closes the system of gas-phase equations.

2.3 Conservation conditions at the liquid/gas interface

At the material interface between liquid and gas, conservation principles apply which represent boundary conditions for the core flow on either side of the interface. For an observer in the laboratory frame, the interface $S(\mathbf{x},t)$ changes position with space and time, and thus a velocity determining that motion must be computed; the change of the interface position will be determined both by liquid rupture (i.e. atomization) and evaporation/condensation. Two ways exist to track an interface. The first way is based on the volume of fluid method (VOF, e.g. [7]) wherein an interface is reconstructed in each computational cell. The problem with this method is that despite being mass-conservative, the method is inaccurate because the interface computed in this manner is necessarily diffuse (i.e. not sharp) since the interface is represented by a cell average; this problem is compounded if there are many species obeying different EOSs [2]. High-order accuracy is difficult to achieve and no VOF scheme having order higher than two exists. Most important, interface properties such as the normal and the curvature are difficult to calculate accurately. This means that there is currently no methodology to utilize the VOF method when evaporation occurs because evaporation occurs normal to the surface, and this aspect is central to our situation. The second way of tracking interfaces relies on the definition of a signed function $G(\mathbf{x}_s,t)$ which defines the interface and is tracked using a level-set method [14]. However, as originally developed, level-set methods are not mass-conservative and much effort has been devoted to mitigating this problem (e.g. [13]). The important advantage of the level set method is that the normal to the surface is inherently part of the model, which makes it natural to adopt it for the present purposes. A comparison between the VOF and level set methods is shown in figure 2.

In the level set method, a scalar $G(\mathbf{x}_s, t)$ is defined such that $G(\mathbf{x_s}, t) = 0$ at the interface, $G(\mathbf{x}, t) > 0$ in the liquid and $G(\mathbf{x}, t) < 0$ in the gas. Function G obeys the equation (e.g. [10])

$$\frac{\partial G}{\partial t} + \mathbf{u} \cdot \nabla G = 0. \tag{20}$$

The conservation conditions at the liquid/gas interface are here written in a laboratory framework and at every location $\mathbf{x}$. The velocity of the interface in the same system of coordinates is denoted by $v_s(\mathbf{x}, t)$ and the normal unit vector to the interface at each location is $\mathbf{n}$. When the interface is tracked by G, then $\mathbf{n} = \nabla G / |\nabla G|$.

We write two types of conservation statements. The first type is made in a small volume across the interface and therefore the values of the dependent variables represent here an average over this control volume. At a much smaller scale, there is a Langmuir-Knudsen layer in which evaporation occurs; for the Langmuir-Knudsen layer, the surface across the interface is so small that it is linear, so that only the dynamics of evaporation counts (i.e. evaporation from a flat interface).

- Mass conservation:

$$\rho_{l,s}(\mathbf{u}_{l,s} \cdot \mathbf{n} - \mathbf{v}_s \cdot \mathbf{n}) = \rho_{g,s}(\mathbf{u}_{g,s} \cdot \mathbf{n} - \mathbf{v}_s \cdot \mathbf{n}) \equiv \dot{m}(\mathbf{x}, t) \tag{21}$$

  where subscript s denotes the interface; $\rho_{l,s} = \rho_l^0$. For an observer in the laboratory frame, equation (21) represents the local rate of mass per unit area per time (g/cm^2-s) transferred between liquid and gas, $\dot{m}(\mathbf{x}, t)$. For evaporation, $\dot{m}(\mathbf{x}, t) > 0$; for condensation, $\dot{m}(\mathbf{x}, t) < 0$. In terms of the molar densities, equation (21) becomes

$$c_{l,s} m_{l,s}(\mathbf{u}_{ls} \cdot \mathbf{n} - \mathbf{v}_s \cdot \mathbf{n}) = c_{g,s} m_{g,s}(\mathbf{u}_{gs} \cdot \mathbf{n} - \mathbf{v}_s \cdot \mathbf{n}). \tag{22}$$

- Momentum conservation:

$$\rho_{l,s}\mathbf{u}_{l,s}(\mathbf{u}_{l,s}\cdot\mathbf{n}-)+p_{l,s}+\mathbf{n}^T\cdot\boldsymbol{\sigma}_{l,s}\cdot\mathbf{n}+\Sigma\kappa = \rho_{g,s}\mathbf{u}_{g,s}(\mathbf{u}_{g,s}\cdot\mathbf{n}-\mathbf{v}_s\cdot\mathbf{n})+p_{g,s}+\mathbf{n}^T\cdot\boldsymbol{\sigma}_{g,s}\cdot\mathbf{n} \tag{23}$$

  where Σ is the surface tension of the liquid, $\kappa = \|\nabla \cdot \mathbf{n}\|$ (the norm of the derivative of the unit tangent vector with respect to the arc length) is the curvature of the interface, $\mathbf{n}^T$ is the transposed of $\mathbf{n}$, and generically

$$\sigma_{ij} = \mu \left(\frac{\partial u_i}{\partial x_j} + \frac{\partial u_j}{\partial x_i} - \frac{2}{3} \frac{\partial u_k}{\partial x_k} \delta_{ij} \right) \tag{24}$$

  with δ_{ij} being the Kronecker symbol. As a note, $\nabla \cdot \mathbf{u}_l = 0$ since $\rho_l = \rho_l^0$.

Σ is function of T and the Eötvös relationship states

$$\Sigma \times \left(\frac{m_{l,s}}{\rho_{l,s}} \right)^{2/3} = \mathcal{K}(T_c - T_l) \tag{25}$$

where $\mathcal{K}$ is a constant having a value valid for almost all substances and T_c is the critical temperature. To minimize complexity, for the purpose of computing the surface tension, we should consider the liquid as an entity rather than as a mixture.

- Conservation of moles of vapor:

$$c_{l,s}(\mathbf{u}_{l,s}\cdot\mathbf{n}-v_s\cdot\mathbf{n}) = c_{g,s}X_{v,s}(\mathbf{u}_{g,s}\cdot\mathbf{n}-v_s\cdot\mathbf{n})+c_{g,s}m_{g,s}\mathcal{D}_{g,s}\left[\nabla\left(\frac{X_v}{m_g}\right)\right]_s\cdot\mathbf{n} \quad (26)$$

  which expresses the conservation of moles and where $X_{ls}=1$ has been used, having assumed that solvability effects of the carrier gas into the liquid are negligible. Diffusion is also occurring in the liquid, but only among individual species; the present conservation statement, equation 26, is for the fuel as an entity and does not take differential diffusivity into account, as already stated in §2.2.

- Energy conservation states that the gas and liquid energy at the surface are equal; this includes heat transfer, latent heat (internal energy is included in the latent heat) and kinetic energy. We make the assumption that there is continuity of temperature at the surface, i.e. $T_{gs}=T_{ls}=T_s$. For a discrete representation of species with k denoting the species and K the total number of species, assuming negligible Soret and Dufour effects, the boundary condition is

$$\dot{m}\left[\frac{(\mathbf{u}_{l,s}\cdot\mathbf{n})^2}{2}-\frac{(\mathbf{u}_{g,s}\cdot\mathbf{n})^2}{2}\right]+\lambda_{l,s}\,\nabla T|_s\cdot\mathbf{n}-\lambda_{g,s}\,\nabla T|_s\cdot\mathbf{n}+p_{l,s}(\mathbf{u}_{\mathbf{l,s}}\cdot\mathbf{n})$$
$$-p_{g,s}(\mathbf{u}_{g,s}\cdot\mathbf{n})+\Sigma\kappa(\mathbf{v}_s\cdot\mathbf{n})=\dot{m}\sum_{k=1}^{K}\left(\frac{h_{kl,s}X_{kl,s}}{m_{l,s}}-\frac{h_{kv,s}X_{kv,s}}{m_{v,s}}\right) \quad (27)$$

  where $h_{kl}=h_k(p_{l,s},T_s,X_{kl,s})$, $h_{kv}=h_k(p_{g,s},T_s,X_{kg,s})$ and $(h_{kv}-h_{kl})=L_v(m_k)$ being the molar heat of evaporation of species k. Note that the kinetic energy term takes into account that the evaporating mass enters the gas phase at a velocity which is that of the liquid surface. Also, the work due to pressure is taken into account, but clearly the work resulting from the force due to surface tension does not enter this statement since that force applies over an interface in contrast to the infinitesimally small control volume (pointwise at the interface) over which these conservation statements are written. Further,

$$\dot{m}\left[\frac{(\mathbf{u}_{l,s}\cdot\mathbf{n})^2}{2}-\frac{(\mathbf{u}_{g,s}\cdot\mathbf{n})^2}{2}\right]+\lambda_{l,s}\,\nabla T|_s\cdot\mathbf{n}-\lambda_{g,s}\,\nabla T|_s\cdot\mathbf{n}+\,p_{l,s}(\mathbf{u}_{l,s}\cdot\mathbf{n})-p_{g,s}(\mathbf{u}_{g,s}\cdot\mathbf{n})$$
$$+\,\Sigma\kappa(\mathbf{v}_s\cdot\mathbf{n})=\dot{m}\sum_{k=1}^{K}\left[L_v(m_k)\frac{X_{kv,s}}{m_{v,s}}+h_{kl}\left(\frac{X_{kv,s}}{m_{v,s}}-\frac{X_{kl,s}}{m_{l,s}}\right)\right] \quad (28)$$

$$\dot{m}\left[\frac{(\mathbf{u}_{l,s}\cdot\mathbf{n})^2}{2}-\frac{(\mathbf{u}_{g,s}\cdot\mathbf{n})^2}{2}\right]+\lambda_{l,s}\,\nabla T|_s\cdot\mathbf{n}-\lambda_{g,s}\,\nabla T|_s\cdot\mathbf{n}\,+p_{l,s}(\mathbf{u}_{l,s}\cdot\mathbf{n})-p_{g,s}(\mathbf{u}_{g,s}\cdot\mathbf{n})$$
$$+\,\Sigma\kappa(\mathbf{v}_s\cdot\mathbf{n})=\dot{m}L_v(m_k)\frac{X_{v,s}}{m_{v,s}}+\dot{m}\sum_{k=1}^{K}h_{kl}\left(\frac{X_{kv,s}}{m_{v,s}}-\frac{X_{kl,s}}{m_{l,s}}\right)\quad(29)$$

In principle, each of the two terms in the sum representing the last term in equation 29 is a joint PDF of h_{kl} and of its multiplier. However, for simplicity, we will assume that the joint PDF can be taken as the product of the marginal PDFs, meaning that the marginal PDFs are uncorrelated. Under this assumption, and with the intention of correlating $h_l(m_k)$, equation 29 becomes

$$\dot{m}\left[\frac{(\mathbf{u}_{l,s}\cdot\mathbf{n})^2}{2}-\frac{(\mathbf{u}_{g,s}\cdot\mathbf{n})^2}{2}\right]+\lambda_{l,s}\,\nabla T|_s\cdot\mathbf{n}-\lambda_{g,s}\,\nabla T|_s\cdot\mathbf{n}+p_{l,s}(\mathbf{u}_{l,s}\cdot\mathbf{n})-p_{g,s}(\mathbf{u}_{g,s}\cdot\mathbf{n})$$
$$+\,\Sigma\kappa(\mathbf{v}_s\cdot\mathbf{n})=\dot{m}L_v(m_k)\frac{X_{v,s}}{m_{v,s}}+\dot{m}h_l(m_k)\left(X_{v,s}P_{v,s}-P_{l,s}\right).\quad(30)$$

In [8], the authors have correlated $h_l(m_k)=\int_0^T C_{pl}dT$ and shown that there is an almost universal curve $C_{pl}/C_{l,bn}$ as a function of T/T_{bn} (subscript bn denotes the normal boiling point). The functional form is

$$C_{pl}/C_{l,bn}=-0.705+4.295(T/T_{bn})-4.20(T/T_{bn})^2+1.61(T/T_{bn})^3\qquad(31)$$

where $0.7\lesssim T/T_{bn}\leqslant 1.35$. In [8] it has also been shown that $C_{l,bn}$ is a function of m_k, $C_{l,bn}=am_k^b$ with a and b being fuel specific (see table 1 from [8]), and that $T_{bn}=A_{bn}\times m_k^{0.5}$, so that it is clear that for every T, $h_l(m_k)$ can be found. The functional form of $C_{l,bn}(m_k)$ and the values of A_{bn} are listed in table 1. Other properties of interest are also listed in that table.

- Individual species conservation through PDF composition-moments conservation (4 equations, assuming the 5th moment is empirically determined as in [9]). For each ξ_n from ξ_1 to ξ_4, the following relationship describes the boundary conditions

$$c_{l,s}(\mathbf{u}_{l,s}\cdot\mathbf{n}-\mathbf{v}_s\cdot\mathbf{n})+c_{l,s}m_{l,s}\mathcal{D}_{l,s}\left[\nabla\left(\frac{\xi_{nl}}{m_l}\right)\right]_s\cdot\mathbf{n}=c_{g,s}X_{v,s}(\mathbf{u}_{g,s}\cdot\mathbf{n}-\mathbf{v}_s\cdot\mathbf{n})$$
$$+\,c_{g,s}m_{g,s}\mathcal{D}_{g,s}\left[\nabla\left(\frac{X_v\xi_{nv}}{m_g}\right)\right]_s\cdot\mathbf{n}.\quad(32)$$

- Thermodynamics of evaporation: This phenomenon occurs in the Knudsen layer, which is at a scale much smaller than that over which the above conservation statements across the layer have been established. Continuos thermodynamics in this context states that the PDFs of the composition on the two

sides of the surface are related, under the ideal-mixture assumption, by Raoult's law (i.e. ideal mixture)

$$P_{v,s} = \frac{p_{vatm}}{X_{v,s} p_{g,s}} P_{l,s} \exp\left[\frac{m_{g,s} L_v(m_v)}{R_u T_b(m_v)}\left(1 - \frac{T_b(m_v)}{T_s}\right)\right], \tag{33}$$

where $p_{vatm} = 1atm$ and $L_v(m_v)$ and $T_b(m_v)$ are the latent heat and the normal boiling point, correlated as functions of m by [9] using Trouton's law,

$$\Delta s_{\text{lg}} = m_v L_v / T_b \simeq 10.6 R_u, \tag{34}$$

and

$$T_b(m_v) = A_b + B_b m_v, \tag{35}$$

where $A_b = 241.4$ and $B_b = 1.45$ for T_b in K (see Appendix A of [11] for more details).

The unknowns to be determined at every point of the interface are: $c_{g,s}$, $c_{l,s}$, $\mathbf{u}_{g,s}\cdot\mathbf{n}$, $\mathbf{u}_{l,s}\cdot\mathbf{n}$, $\mathbf{v}_s\cdot\mathbf{n}$, $X_{v,s}$, $p_{g,s}$, $p_{l,s}$, T_s, $\theta_{v,s}$, $\theta_{l,s}$, $\psi_{v,s}$, $\psi_{l,s}$, $\xi_{3v,s}$, $\xi_{3l,s}$, $\xi_{4g,s}$, $\xi_{4l,s}$. There are 17 unknowns. There are also 8 conservation statements across the boundaries and 1 relationship emerging from the Knudsen layer analysis; a total of 9 equations. The remaining 8 equations are the liquid momentum conservation equation, liquid energy equation, 4 liquid moment equations for the composition, the liquid equation of state $\rho_l = \rho_l^o$, and the perfect gas equation of state for the gas, all of which must be satisfied at the interface.

3 Analysis

We address here some of the most pertinent questions that must be asked when faced with a new model. This analysis is inspired by the fluid mechanics similarity principle of [1] which states that if non-dimensional numbers can be defined in differential equations, then, independent of transport properties and dependent variables values, flows with the same value of a specific non-dimensional number behave in the same manner with respect to the quantities measured by the specific non-dimensional number. Since composition equations were never analyzed in this manner in the past, we first wish to know if one can define effective compositional Schmidt numbers, $\text{Sc}_{\xi nl,eff}$ and $\text{Sc}_{\xi nv,eff}$, which would provide insights on the length scales associated with the moments of the composition compared to those of viscosity changes. The Schmidt number, $\text{Sc} = \mu/\rho\mathcal{D}$, is usually defined in connection with the species mass fraction equation and measures the relative importance of transport of momentum with respect to transport of species mass, but, as stated above, there is no equivalent definition of transport of momentum and *transport of composition rather than species mass* (transport of species mass only involves one species rather than the ensemble

of the species as addressed by the composition). This information would be of interest because it would provide an estimate of the flow dynamics with respect to the composition and indicate which length scale is likely to be shorter; this is an essential aspect of this work. Second, since one of the major differences between the present formulation and the previous ones is the concomitant evaporation that accompanies liquid atomization, understanding the important dependencies which are involved in heat transfer from the gas to the liquid that govern liquid heating and thus evaporation is one of the highlights of the analysis. Thus, we inquire about the heat transfer length scale by reformulating the heat flux in the energy equation so as to enable the identification of an effective gas Prandtl number, $\mathrm{Pr}_{g,eff}$.

Knowing the values of these non-dimensional numbers for given fuels and under specified initial conditions would provide a quick indication to design engineers as to what to expect in terms of the prevailing phenomenon - atomization faster than phase change or vice versa - and thus guide them in their design.

3.1 Reformulation of the compositional fluxes to define $\mathbf{Sc}_{\xi nl,eff}$ and $\mathbf{Sc}_{\xi nv,eff}$

We first perform the analysis for the vapor composition equations because they are more complex, and then we will present the simpler result for the liquid.

Considering the fluxes in the moment composition equations

$$J_{\xi nv,j} = -c_g m_g \mathcal{D}_{g,\xi n} \frac{\partial}{\partial x_j}\left(\frac{X_v \xi_{nv}}{m_g}\right)$$

we wish to identify $\mathrm{Sc}_{\xi nv,eff}$ which is defined as

$$\mathrm{Sc}_{\xi nv,eff} \equiv \frac{\mu_g}{\rho_g \mathcal{D}_{\xi nv,eff}} \tag{36}$$

$$J_{\xi nv,j} = -\mathcal{D}_{\xi nv,eff} \frac{\partial \xi_{nv}}{\partial x_j} \tag{37}$$

where $J_{\xi nv,j}$ is the flux of moment ξ_{nv} in the j^{th} direction. From the definition of $\mathrm{Sc}_{\xi nv,eff}$, it is clear that if $\mathrm{Sc}_{\xi nv,eff} < 1$, then the time scale over which the composition changes will be larger than the time scale over which viscosity changes, which means that the gas evolved from evaporation will have similar composition to the liquid. If $\mathrm{Sc}_{\xi nv,eff} > 1$, the gas composition will be drastically different from that of the liquid.

By noting that all variables representing the elements of vector Φ (see equation (14)) are related through the solution of the set of governing equations, we can write

$$X_v = f_0(\mathbf{x},t), \quad \theta_v = f_1(\mathbf{x},t), \quad \psi_v = f_2(\mathbf{x},t), \quad \xi_{3v} = f_3(\mathbf{x},t), \quad \xi_{4v} = f_4(\mathbf{x},t) \tag{38}$$

where f_m $m \in [0,4]$ are representative functions, and similarly

$$T = f_T(\mathbf{x},t) \text{ and } p = f_p(\mathbf{x},t). \tag{39}$$

Under the assumption that

$$X_v = g(f_T(\mathbf{x},t)), \quad \theta_v = l(f_T(\mathbf{x},t)), \quad \text{etc.} \tag{40}$$

where g, l etc. are composite functions, one can write

$$\frac{\partial X_v}{\partial x_j} = \frac{\partial g(f_T(\mathbf{x},t))}{\partial x_i} = \frac{\delta g(f_T(\mathbf{x},t))}{\delta f_T(\mathbf{x},t)} \frac{\partial f_T(\mathbf{x},t)}{\partial x_i} \tag{41}$$

where δ denotes a functional derivative; similar expression hold for all other variables. The assumption of equation (40) is expected to hold in regions of large gradients, i.e. where there is substantial compositional and heat activity (i.e. changes). Then,

$$\begin{aligned} c_g m_g \mathcal{D}_{g,\xi n} \frac{\partial}{\partial x_j}\left(\frac{X_v \xi_{nv}}{m_g}\right) &= c_g m_g \mathcal{D}_{g,\xi n}\left(\frac{\xi_{nv}}{m_g}\frac{\partial X_v}{\partial x_j} + \frac{X_v}{m_g}\frac{\partial \xi_{nv}}{\partial x_j} - \frac{X_v \xi_{nv}}{m_g^2}\frac{\partial m_g}{\partial x_j}\right) \\ &= c_g m_g \mathcal{D}_{g,\xi n}\left(\frac{\xi_{nv}}{m_g}\frac{\delta X_v}{\delta \xi_{nv}} + \frac{X_v}{m_g} - \frac{X_v \xi_{nv}}{m_g^2}\frac{\delta m_g}{\delta \xi_{nv}}\right)\frac{\partial \xi_{nv}}{\partial x_j} \\ &= c_g m_g \mathcal{D}_{g,\xi n}\left(\frac{\xi_{nv}}{m_g}\frac{\delta X_v}{\delta \xi_{nv}} + \frac{X_v}{m_g} - \frac{X_v \xi_{nv}}{m_g^2}\frac{\delta m_g}{\delta X_v}\frac{\delta X_v}{\delta \xi_{nv}}\right)\frac{\partial \xi_{nv}}{\partial x_j} \end{aligned} \tag{42}$$

which considering equation (16) showing that $\frac{\delta m_g}{\delta X_v} = \theta_v - m_a$, leads to

$$c_g m_g \mathcal{D}_{g,\xi n} \frac{\partial}{\partial x_j}\left(\frac{X_v \xi_{nv}}{m_g}\right) = c_g m_g \mathcal{D}_{g,\xi n}\left[\left(1 - \frac{X_v}{m_g}(\theta_v - m_a)\right)\frac{\xi_{nv}}{m_g}\frac{\delta X_v}{\delta \xi_{nv}} + \frac{X_v}{m_g}\right]\frac{\partial \xi_{nv}}{\partial x_j}. \tag{43}$$

Thus, comparing equations (37) and (43) one obtains

$$\mathcal{D}_{\xi nv,eff} = c_g m_g \mathcal{D}_{g,\xi n}\left[\left(1 - \frac{X_v}{m_g}(\theta_v - m_a)\right)\frac{\xi_{nv}}{m_g}\frac{\delta X_v}{\delta \xi_{nv}} + \frac{X_v}{m_g}\right]. \tag{44}$$

Equation (44) indicates that additional to the algebraic dependencies of $\mathcal{D}_{\xi nv,eff}$ on the dependent variables c_g, m_g, X_v, θ_v and ξ_{nv}, and on the diffusion coefficient $\mathcal{D}_{g,\xi n}$ defined by equation (18), the variation of the vapor mole fraction with respect to the PDF's n^{th} moment is what most determines the variation of $\mathcal{D}_{\xi nv,eff}$. This variation will be most likely fuel dependent and initial-conditions dependent. Once simulations become available, $\frac{\delta X_v}{\delta \xi_{nv}}$ can be modeled and this model evaluated by comparisons with the database obtained from the simulations. Such a model would enable the calculation of $\mathcal{D}_{\xi nv,eff}$ and further of $\mathrm{Sc}_{\xi nv,eff}$, which would be very helpful for design engineers.

For the liquid, a similar derivation leads to

$$c_l m_l \mathcal{D}_{g,\xi n} \frac{\partial}{\partial x_j}\left(\frac{\xi_{nl}}{m_l}\right) = c_l m_l \mathcal{D}_{l,\xi n}\left(\frac{1}{m_l} - \frac{1}{m_l^2}\frac{\delta m_l}{\delta \xi_{nl}}\right)\frac{\partial \xi_{nl}}{\partial x_j}, \tag{45}$$

$$\mathcal{D}_{\xi nl,eff} = c_l m_l \mathcal{D}_{l,\xi n}\left(\frac{1}{m_l} - \frac{1}{m_l^2}\frac{\delta m_l}{\delta \xi_{nl}}\right), \tag{46}$$

$$\mathrm{Sc}_{\xi nl,eff} \equiv \frac{\mu_l}{\rho_l \mathcal{D}_{\xi nl,eff}} \tag{47}$$

and the same comments as for $\mathrm{Sc}_{\xi nv,eff}$ apply regarding the usefulness in knowing the range of values of this number. Equation 46 shows that in addition to c_l, m_l and $\mathcal{D}_{l,\xi n}$ as defined by equation 11, the variation of $\mathcal{D}_{\xi nl,eff}$ is most influenced by the variation of the liquid molar with respect to the n^{th} moment of the liquid-composition PDF. From the definition of $\mathrm{Sc}_{\xi nl,eff}$, it is clear that if $\mathrm{Sc}_{\xi nl,eff} < 1$, then the time scale over which the composition changes will be larger than the time scale over which viscosity changes, which means that the drops resulting from atomization will have similar composition to the liquid from which they originate. If $\mathrm{Sc}_{\xi nl,eff} > 1$, the drop composition will be drastically different from that of the liquid from which they originate.

3.2 Reformulation of the gas heat flux identify $\mathbf{Pr}_{g,eff}$

From equation (15), the gas heat flux in the j direction is

$$q_{g,j} = \lambda_g \frac{\partial T_g}{\partial x_j} + \alpha_1(T_g)\frac{\partial}{\partial x_j}\left(\frac{X_v}{m_g}\right) + \alpha_2(T_g)\frac{\partial}{\partial x_j}\left(\frac{X_v \theta_v}{m_g}\right) + \alpha_3 \frac{\partial}{\partial x_j}\left(\frac{X_v \psi_v}{m_g}\right) \tag{48}$$

which is not conducive to identifying $\mathrm{Pr}_{g,eff}$ defined as

$$\mathrm{Pr}_{g,eff} \equiv \frac{C_{p,g}\mu_g}{\Lambda_{g,eff}}, \tag{49}$$

$$q_{g,j} = \frac{\partial}{\partial x_j}\left(\Lambda_{g,eff}\frac{\partial T_g}{\partial x_j}\right). \tag{50}$$

If $\mathrm{Pr}_{g,eff} < 1$, then the heat transfer characteristic time will be much larger than that of momentum transfer, which means that liquid heating will be secondary compared to the mechanical forces determining atomization;and the opposite will happen if $\mathrm{Pr}_{g,eff} > 1$.

Using the above formalism and the assumption of equation (40), the second term

of equation (50) can be written as

$$\alpha_1(T_g)\frac{\partial}{\partial x_j}\left(\frac{X_v}{m_g}\right)=\alpha_1(T_g)\frac{\partial}{\partial T_g}\left(\frac{X_v}{m_g}\right)\frac{\partial T_g}{\partial x_j}=\alpha_1(T_g)\left[\frac{1}{m_g}\frac{\partial X_v}{\partial T_g}+X_v\frac{\partial}{\partial T_g}\left(\frac{1}{m_g}\right)\right]\frac{\partial T_g}{\partial x_j} \tag{51}$$

$$=\alpha_1(T_g)\left[\frac{1}{m_g}\frac{\delta X_v}{\delta T_g}-\frac{1}{m_g^2}X_v\frac{\delta m_g}{\delta T_g}\right]\frac{\partial T_g}{\partial x_j} \tag{52}$$

$$=\alpha_1(T_g)\left\{\frac{1}{m_g}\frac{\delta X_v}{\delta T_g}-\frac{X_v}{m_g^2}\left[-m_{ag}\frac{\delta X_v}{\delta T_g}+\theta_v\frac{\delta X_v}{\delta T_g}+X_v\frac{\delta\theta_v}{\delta T_g}\right]\right\}\frac{\partial T_g}{\partial x_j} \tag{53}$$

$$=\alpha_1(T_g)\left\{\left[\frac{1}{m_g}+\frac{X_v}{m_g^2}(m_{ag}-\theta_v)\right]\frac{\delta X_v}{\delta T_g}-\frac{X_v^2}{m_g^2}\frac{\delta\theta_v}{\delta T_g}\right\}\frac{\partial T_g}{\partial x_j}. \tag{54}$$

Using the same method for the other terms one obtains

$$\alpha_2(T_g)\frac{\partial}{\partial x_j}\left(\frac{X_v\theta_v}{m_g}\right)=\alpha_2(T_g)\left\{\frac{\partial}{\partial T_g}\left(\frac{X_v\theta_v}{m_g}\right)\frac{\partial T_g}{\partial x_j}\right\}=\alpha_2(T_g)\left\{\theta_v\frac{\partial}{\partial T_g}\left(\frac{X_v}{m_g}\right)+\frac{X_v}{m_g}\frac{\partial\theta_v}{\partial T_g}\right\}\frac{\partial T_g}{\partial x_j} \tag{55}$$

$$=\alpha_2(T_g)\left\{\theta_v\left[\frac{1}{m_g}\frac{\delta X_v}{\delta T_g}-\frac{X_v}{m_g^2}\left(-m_{ag}\frac{\delta X_v}{\delta T_g}+\theta_v\frac{\delta X_v}{\delta T_g}+X_v\frac{\delta\theta_v}{\delta T_g}\right)\right]+\frac{X_v}{m_g}\frac{\delta\theta_v}{\delta T_g}\right\}\frac{\partial T_g}{\partial x_j} \tag{56}$$

$$=\alpha_2(T_g)\left\{\theta_v\left[\frac{1}{m_g}+\frac{X_v}{m_g^2}(m_{ag}-\theta_v)\right]\frac{\delta X_v}{\delta T_g}+\left(\frac{X_v}{m_g}-\theta_v\frac{X_v^2}{m_g^2}\right)\frac{\delta\theta_v}{\delta T_g}\right\}\frac{\partial T_g}{\partial x_j}, \tag{57}$$

and

$$\alpha_3\frac{\partial}{\partial x_j}\left(\frac{X_v\psi_v}{m_g}\right)=\alpha_3\left\{\psi_v\left[\frac{1}{m_g}\frac{\delta X_v}{\delta T_g}-\frac{X_v}{m_g^2}\left(-m_{ag}\frac{\delta X_v}{\delta T_g}+\psi_v\frac{\delta X_v}{\delta T_g}+X_v\frac{\delta\psi_v}{\delta T_g}\right)\right]+\frac{X_v}{m_g}\frac{\delta\psi_v}{\delta T_g}\right\}\frac{\partial T_g}{\partial x_j} \tag{58}$$

$$=\alpha_3\left\{\psi_v\left[\frac{1}{m_g}+\frac{X_v}{m_g^2}(m_{ag}-\psi_v)\right]\frac{\delta X_v}{\delta T_g}+\left(\frac{X_v}{m_g}-\psi_v\frac{X_v^2}{m_g^2}\right)\frac{\delta\psi_v}{\delta T_g}\right\}\frac{\partial T_g}{\partial x_j}. \tag{59}$$

This gives

$$\begin{aligned}\Lambda_{g,eff}=\lambda_g&+\left\{\left(\alpha_1(T_g)+\theta_v\alpha_2(T_g)\right)\left[\frac{1}{m_g}+\frac{X_v}{m_g^2}(m_{ag}-\theta_v)\right]+\alpha_3\psi_v\left[\frac{1}{m_g}+\frac{X_v}{m_g^2}(m_{ag}-\psi_v)\right]\right\}\frac{\delta X_v}{\delta T_g}\\&+\left[\alpha_2(T_g)\left(\frac{X_v}{m_g}-\theta_v\frac{X_v^2}{m_g^2}\right)-\alpha_1(T_g)\frac{X_v^2}{m_g^2}\right]\frac{\delta\theta_v}{\delta T_g}\\&+\alpha_3\left(\frac{X_v}{m_g}-\psi_v\frac{X_v^2}{m_g^2}\right)\frac{\delta\psi_v}{\delta T_g}.\end{aligned} \tag{60}$$

It is thus clear that the effective thermal conductivity, $\Lambda_{g,eff}$, is highly dependent both upon the variation of the vapor molar fraction with T through $\frac{\delta X_v}{\delta T_g}$ and upon the composition variation with T through $\frac{\delta \theta_v}{\delta T_g}$ and $\frac{\delta \psi_v}{\delta T_g}$. Once numerical solutions of the governing equations will be obtained, models for these gradient variations should be sought and evaluated using the database so as to enable the computation of $\mathrm{Pr}_{g,eff}$. Such a model will give an indication to design engineers as to the prevailing influence between heating and viscous effects.

For the liquid, a similar derivation leads to

$$\alpha_1(T_l)\frac{\partial}{\partial x_j}\left(\frac{1}{m_l}\right) = \alpha_1(T_l)\left(-\frac{1}{m_l^2}\frac{\delta m_l}{\delta T_l}\right)\frac{\partial T_l}{\partial x_j} \tag{61}$$

$$\alpha_2(T_l)\frac{\partial}{\partial x_j}\left(\frac{\theta_l}{m_l}\right) = \alpha_2(T_l)\left(\frac{1}{m_l}\frac{\delta \theta_l}{\delta T_l} - \frac{\theta_l}{m_l^2}\frac{\delta m_l}{\delta T_l}\right)\frac{\partial T_l}{\partial x_j} \tag{62}$$

$$\alpha_3(T_l)\frac{\partial}{\partial x_j}\left(\frac{\psi_l}{m_l}\right) = \alpha_3(T_l)\left(\frac{1}{m_l}\frac{\delta \psi_l}{\delta T_l} - \frac{\psi_l}{m_l^2}\frac{\delta m_l}{\delta T_l}\right)\frac{\partial T_l}{\partial x_j} \tag{63}$$

with the result that

$$\Lambda_{l,eff} = \lambda - \frac{1}{m_l^2}\frac{\delta m_l}{\delta T_l}\left[\alpha_1(T_l) + \alpha_2(T_l)\theta_l + \alpha_3(T_l)\psi_l\right] + \frac{1}{m_l}\left[\alpha_2(T_l)\frac{\delta \theta_l}{\delta T_l} + \alpha_3(T_l)\frac{\delta \psi_l}{\delta T_l}\right] \tag{64}$$

$$\mathrm{Pr}_{l,eff} = \frac{C_{p,l}\mu_l}{\Lambda_{l,eff}} \tag{65}$$

showing that beside the first and second moment of the composition variation with the temperature, the variation of the molar mass with temperature due to changes in the liquid composition resulting from phase change mostly affect the effective thermal conductivity of the liquid. This result is intuitively correct and give confidence in the model, while prospective future simulations may be used to evaluate future models of $\frac{\delta m_l}{\delta T_l}$, $\frac{\delta \theta_l}{\delta T_l}$ and $\frac{\delta \psi_l}{\delta T_l}$ for utilization of $\Lambda_{l,eff}$ and $\mathrm{Pr}_{l,eff}$ by design engineers.

4 Summary and conclusions

A new formulation has been developed for describing the concurrent atomization and phase change of a fully multicomponent liquid. Additional to the conventional governing equations, the composition is tracked for both liquid and surrounding gas. With computational efficiency in mind, the composition is statistically described by a distribution function parametrized on the molar mass. The surface between liquid and gas is tracked using a level-set method as being the sole existing method to allow the accurate definition of a normal to the surface that is necessary to compute evaporation.

An analysis of the governing equations focussed on quantities which, when computed from a database produced through simulations, will be of help to engineers.

As such, we have defined novel non-dimensional numbers evaluating the relative importance of the composition versus viscosity which is a property governing surface tension; knowing whether compositional or viscous effects are faster will be of help in understanding how close will the composition of drops be with respect to the original fuel. Moreover, an effective Prandtl number has also been derived to evaluate the ratio of the characteristic times of heat conduction, which is instrumental to phase change, and viscosity which governs atomization. The functional dependency of these numbers on the dependent variables and their relative variation with respect to each other has been shown and discussed.

Appendix 1: Calculation of the portion of the heat flux that is due to transport of molar fluxes

Details of the heat flux in equation (15) are as follows:

$$\alpha_1(T) = R_u A_p (A_b - T) - \Delta s_{\text{lg}} A_b \tag{66}$$

$$\alpha_2(T) = (C_{p,a} - R_u B_p) T + R_u (A_b B_p + A_c B_b) - \Delta s_{\text{lg}} B_b - C_l A_b \tag{67}$$

$$\alpha_3 = B_b [R_u B_p - C_{pl}] \tag{68}$$

where $C_{p,a} = \gamma_{ther,a} R_u / (\gamma_{ther,a} - 1) m_a$ (kJ/(kg K)) is the air heat capacity at constant pressure, $m_a = 29$ kg/kmol, $\gamma_{ther,a} = 1.4$ is the ratio of gas heat capacities, $\Delta s_{\text{lg}} = m L_v / T_b$ where L_v is the latent heat and T_b is the normal boiling point, $R_u = 8.3142$ (kJ/(kmol K)) and

$$C_{pg}(m) = (A_p + B_p m) R_u / m \quad \text{in (kJ/(kgK))}, \tag{69}$$

is the gas heat capacity where $A_p = 2.465 - 1.144 \times 10^{-2} T_r + 1.759 \times 10^{-5} T_r^2 - 5.972 \times 10^{-9} T_r^3$ and $B_p = -0.03561 + 9.367 \times 10^{-4} T_r - 6.030 \times 10^{-7} T_r^2 + 1.324 \times 10^{-10} T_r^3$ (see [3]) with the reference temperature T_r being that of [12]

$$\text{Pr} = 0.815 - 4.958 \times 10^{-4} T_{ref} + 4.515 \times 10^{-7} T_{ref}^2 \tag{70}$$

$$T_{ref} = (2/3) T_{ls} + (1/3) T \tag{71}$$

leading to Pr values of 0.696, 0.694 and 0.693 for $T = 375$ K, 400 K and 425 K, respectively. Following [16], $C_{pl} = 2.26 - 2.94 \times 10^{-3} T_{r,l} + 9.46 \times 10^{-6} T_{r,l}^2$ (kJ/kgK) where $T_{r,l} = T_l / T_{cr,l}$. Constants A_b and B_b are defined in §2.3.

More details and transport property values are given in Appendix A of [11].

Acknowledgements

This work was conducted at the Jet Propulsion Laboratory (JPL), California Institute of Technology (Caltech) and sponsored by NASA under the ARMD Seedling Program.

References

[1] Batchelor, G. K. 1999 *An Introduction to Fluid Dynamics,* Cambridge University Press.

[2] Chertock, A., Karni, S. & Kurganov, A. 2008 Interface tracking method for compressible multifluids. *ESAIM: M2AN.* **42**, 991-1019.

[3] Chou, G. F. & Prausnitz , J. M. 1986 Adiabatic flash calculations for continuous or semicontinuous mixtures using an equation of state. *Fluid Phase Equilibria* **30**, 75-82.

[4] Cotterman, R. L., Bender R. & Prausnitz J. M. 1985 Phase equilibria for mixtures containing very many components. Development and application of continuous thermodynamics for chemical process design. *Ind. Eng. Chem. Process Des. Dev.* **24**, 194–203.

[5] Edwards, T. & Maurice L. Q. 2001 Surrogate mixtures to represent complex aviation and rocket fuels. *J. Propul. Power* **17**(2), 461-466.

[6] B. Gal-Or, B., Cullinan, Jr., H. T. & Galli, R. 1975 New thermodynamic-transport theory for systems with continuous component density distributions. *Chem. Eng. Sci.* **30**, 1085-1092.

[7] Gueyffier, D., Li, J., Nadim, A., Scardovelli, R. & Zaleski, S. 1999 Volume-of-fluid interface tracking with smoothed surface stress methods for three-dimensional flows. *J. Comp. Phys.* **152**, 423-456.

[8] Harstad, K. & Bellan, J. 2004 Modeling evaporation of Jet A, JP-7 and RP-1 drops at 1 to 15 bars. *Combust. Flame* **137**(1-2), 163-177.

[9] Harstad, K. G., Le Clercq, P. C. & Bellan, J. 2003 A statistical model of multicomponent-fuel drop evaporation for many-droplet gas-liquid flow simulations, AIAA J. **41**(10), 1858-1874.

[10] Herrmann, M. 2008 A balanced force refined level set grid method for two-phase flows on unstructured flow solver grids. *J. Comp. Phys.* **227**, 2674-2706.

[11] Le Clercq, P. C. & Bellan, J. 2003 Direct numerical simulation of gaseous mixing layers laden with multicomponent-liquid drops: Liquid-specific effects. *J. Fluid Mech.* **533**, 57-94.

[12] Miller, R. S., Harstad, K. & Bellan, J. 1998 Evaluation of equilibrium and non-equilibrium evaporation models for many-droplet gas-liquid flow simulations. *Int. J. Multiphase Flow* **24**, 1025-1055.

[13] Olsson, E. & Kreiss, G. 2005 A conservative level set method for two phase flow. *J. Comp. Phys* **210**(1), 225–246.

[14] Osher, S. & Sethian, J. A. 1988 Fronts propagating with curvature-dependent speed: Algorithms based on Hamilton-Jacobi formulations. *J. Comput. Phys.* 79, 12–49.

[15] Rätzsch, M. T. & Kehlen, H. 1983 Continuous thermodynamics model of complex mixtures. *Fluid Phase Equilibria* **14**, 225-234.

[16] Tamim, J. and Hallett, W. L. H. 1995 A continuous thermodynamics model for multicomponent droplet vaporization. *Chem. Eng. Sci.* **50**, 2933-2942.

[17] Whitson, C. H. 1983 Characterizing hydrocarbon plus fractions. *Soc. Pet. Eng. J.* **23**, 683-694.

[18] Zhao, Y. & Qiu, H. H. 2006 Measurements of multicomponent microdroplet evaporation by using Rainbow Refractometer and PDA. *Exp. Fluids* **40**, 60-69.

Property	Hydrocarbon					
	n-alkane	naphthene	aromatic	Jet A	JP-7	RP-1
A_{bn} $(\mathrm{mol/g})^{0.5}\mathrm{K}$	37.1	$38^{[+1.0;-0.5]}$	$40^{[+2.0;-0.5]}$	38	37.5	37.7
λ_{vbn} $(\mathrm{W/mK}) \times 10^3$	$2.01m^{0.48}$	$0.378m^{0.84}$	$0.74m^{0.68}$	$1.138m^{0.60}$	$1.158m^{0.60}$	$0.726m^{0.70}$
$C_{vbn}(\mathrm{J/gK})$	$0.39\ m^{0.36}$	$0.07\ m^{0.70}$	$0.099\ m^{0.60}$	$0.186\ m^{0.50}$	$0.192\ m^{0.50}$	$0.116\ m^{0.60}$
C_{lbn} $(\mathrm{J/gK})$	$0.75\ m^{0.26}$	$0.317\ m^{0.42}$	$0.32m^{0.40}$	$0.485\ m^{0.34}$	$0.485\ m^{0.34}$	$0.485\ m^{0.34}$
ρ_{lbn} $(\mathrm{g/cm^3})$	0.60	0.715	0.78	0.665	0.65	0.67
ρ_c $(\mathrm{g/cm^3})$	0.233	0.27	0.29	0.25	0.25	0.25

Table 1: Properties of hydrocarbon classes and kerosene fuels. Exponents in brackets denote the error range. From [8].

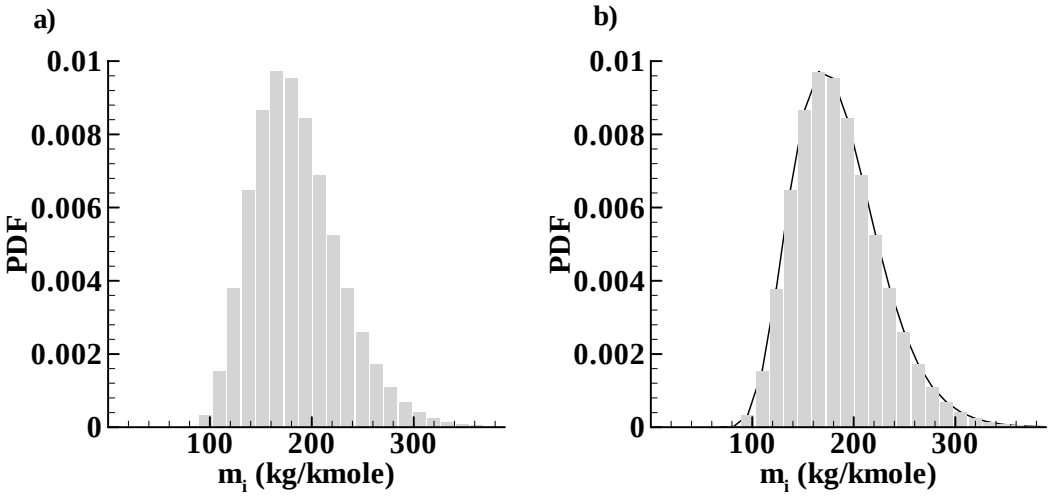

Figure 1. Discrete composition Probability Distribution Function (PDF) given as a discrete 'bar chart' of mole fractions (a) and continuous PDF (solid line) fitted on the discrete chart (b).

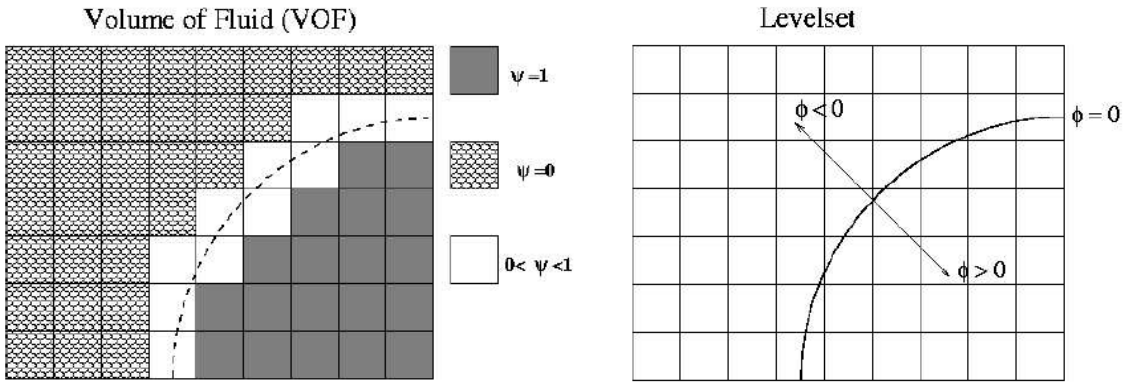

Figure 2. Comparison between the Volume of Fluid (VOF) method (left) and the Level Set method (right).